AAC
Journals.ASM.org

Interaction of Silver Nanoparticles with Serum Proteins Affects Their Antimicrobial Activity *In Vivo*

Divya Prakash Gnanadhas,[a,b] Midhun Ben Thomas,[a,c] Rony Thomas,[a] Ashok M. Raichur,[c,d] Dipshikha Chakravortty[a]

Department of Microbiology and Cell Biology, Indian Institute of Science, Bangalore, India[a]; Department of Aerospace Engineering, Indian Institute of Science, Bangalore, India[b]; Department of Materials Engineering, Indian Institute of Science, Bangalore, India[c]; Department of Applied Chemistry, University of Johannesburg, Doornfontein, South Africa[d]

The emergence of multidrug-resistant bacteria is a global threat for human society. There exist recorded data that silver was used as an antimicrobial agent by the ancient Greeks and Romans during the 8th century. Silver nanoparticles (AgNPs) are of potential interest because of their effective antibacterial and antiviral activities, with minimal cytotoxic effects on the cells. However, very few reports have shown the usage of AgNPs for antibacterial therapy *in vivo*. In this study, we deciphered the importance of the chosen methods for synthesis and capping of AgNPs for their improved activity *in vivo*. The interaction of AgNPs with serum albumin has a significant effect on their antibacterial activity. It was observed that uncapped AgNPs exhibited no antibacterial activity in the presence of serum proteins, due to the interaction with bovine serum albumin (BSA), which was confirmed by UV-Vis spectroscopy. However, capped AgNPs [with citrate or poly(vinylpyrrolidone)] exhibited antibacterial properties due to minimized interactions with serum proteins. The damage in the bacterial membrane was assessed by flow cytometry, which also showed that only capped AgNPs exhibited antibacterial properties, even in the presence of BSA. In order to understand the *in vivo* relevance of the antibacterial activities of different AgNPs, a murine salmonellosis model was used. It was conclusively proved that AgNPs capped with citrate or PVP exhibited significant antibacterial activities *in vivo* against *Salmonella* infection compared to uncapped AgNPs. These results clearly demonstrate the importance of capping agents and the synthesis method for AgNPs in their use as antimicrobial agents for therapeutic purposes.

In the last decade, nanotechnology has emerged as one of the fastest growing areas of science and technology. Its wide array of applications in various fields as diverse as agriculture, electronics, and the military is a testament to this exponential growth. But what makes nanotechnology all the more appealing are the numerous advantages it provides to the medical sector, such as the roles of nanoparticles in drug delivery, molecular imaging, and therapy, as well as the development of materials and devices with antimicrobial properties (1–3).

Since the 18th century, silver in the form of silver nitrate, silver sulfadiazine, etc., has been in use for the treatment of burns, wounds, and other bacterial infections (4–6). This property led to silver being incorporated into various bactericidal applications. Numerous methods have been formulated for the synthesis of AgNPs, such as reduction of silver ions on the surface of functionalized silica (7, 8), silver ions reduced in mesoporous silica, and in the presence of stabilizers in aqueous solution (9) leading to the formation of silver-incorporated nanoparticles. Nanoparticles have come to the forefront due to their distinctive physical, chemical, and biological properties, which arise from their high surface area-to-mass ratio (10, 11). Various methods have been adapted for the synthesis of AgNPs, and the antibacterial activities of the AgNPs vary with the different synthesis methods. Capping agents are also used for the stabilization of the nanoparticles, and the capped AgNPs exhibit better antibacterial activity than uncapped AgNPs (12–14). Although the antibacterial properties of silver ions are well established, there are various hypotheses regarding the mechanism of action. There have been reports that the deposition of silver on the cell wall affects the permeability (15) and formation of electron-dense granules (16, 17). Other studies have indicated the inability of DNA to replicate after treatment with silver ions and the inactivation of enzymes via reaction with thiol groups (18, 19). *Vibrio cholerae* and *Escherichia coli* experience a massive proton leakage through the membrane that leads to the collapse of the proton motive force (20, 21). AgNPs display potent antibacterial and bactericidal properties, not only against Gram-positive and Gram-negative bacteria in general but also against methicillin-resistant bacterial strains (22). AgNPs have been found to exhibit antibacterial activities at a very low concentration (1.69 μg/ml) and exhibit synergistic activities with different classes of antibiotics, such as β-lactams (penicillin and amoxicillin), lincosamides (clindamycin), and macrolides (erythromycin) (23). Studies have proved that the antibacterial efficacies of AgNPs are size and shape dependent, with truncated triangular shapes showing bacterial inhibition with a silver content of 1 μg, while 12.5 μg and 50 to 100 μg required for spherical and rod-shaped particles, respectively (5, 24). Similarly, size was also found to play a significant role, as more particles come in contact with the bacterial cells when there is a large total surface area (25).

The action of AgNPs evokes inflammatory responses in the host due to the generation of reactive oxygen species (ROS). This in turn induces oxidative stress, which leads to apoptosis and an increase in the transcription of proinflammatory cytokines due to

Received 19 March 2013 Returned for modification 19 April 2013
Accepted 18 July 2013
Published ahead of print 22 July 2013
Address correspondence to Dipshikha Chakravortty, dipa@mcbl.iisc.ernet.in.
Supplemental material for this article may be found at http://dx.doi.org/10.1128/AAC.00152-13.

doi:10.1128/AAC.00152-13

activation of the c-Jun N-terminal kinase pathway (26). In spite of all these advantages, various studies have found that long-term use of a low concentration of silver ions in wound dressings can lead to increased resistance of *Staphylococcus aureus* to silver (27).

One of the major health issues of the modern world is the danger posed by food-borne diseases, for which *Salmonella enterica* is one of the most prevalent agents. *Salmonella enterica* is a Gram-negative, intracellular, non-spore-forming bacillus of the *Enterobacteriaceae* family and causes a wide array of symptoms, such as gastroenteritis, bacteremia, and typhoid fever (28). These bacteria translocate across the epithelial cells via a *Salmonella* pathogenicity island 1 (SPI 1)-dependent mechanism, after which they infect macrophages and, prior to dissemination, remain inside vacuoles (29, 30). Among the numerous drugs in vogue, fluoroquinolones, such as ciprofloxacin, and broad-spectrum cephalosporins, such as ceftriaxone and ceftiofur, are the drugs of choice to combat typhoid fever. The MIC of ciprofloxacin for *S. enterica* serovar Typhimurium ATCC 14028 is ~0.02 μg/ml, and *Salmonella* strains having MICs of <1 μg/ml are categorized as susceptible strains. The biggest bane in the present scenario is the emergence of multidrug-resistant *Salmonella* (31–33). Recent studies have demonstrated that the AgNPs exhibited antibacterial properties by virtue of the generation of ROS at the contact surfaces (34–36). Nevertheless, very few studies have shown the usage of AgNPs as a therapeutic agent *in vivo* (37–39). In this study, we demonstrate an important phenomenon of interaction of AgNPs with serum proteins, which hinder the antibacterial properties of these particles. Further, we demonstrate that use of capping agents reduces the particles' interactions and restores their antibacterial activity. The potency of AgNPs is based on the type of capping agent used.

MATERIALS AND METHODS

The chemicals used in this study were purchased from Sigma-Aldrich unless otherwise mentioned.

Synthesis of silver nanoparticles. (i) Chemical reduction method. Uncapped AgNPs were prepared by reducing Ag^{1+} to Ag^0 (40). Briefly, 1 mM $AgNO_3$ solution was added dropwise to 2 mM $NaBH_4$ at 4°C with vigorous stirring at 300 rpm. The change of color to golden yellow (due to surface plasmon resonance) indicated the formation of AgNPs. The presence of a typical plasmon resonance peak in the wavelength range of 380 to 420 nm confirmed the formation of AgNPs. In order to ensure the reduction of all silver ions, an excess amount of reducing agent ($NaBH_4$) was used. Subsequently, AgNPs were dialyzed (2-kDa cutoff) to remove any traces of other compounds. Energy dispersive analysis using X-rays was performed during scanning electron microscopic (SEM) analysis to check the purity of the nanoparticles.

(ii) Citrate-capped silver nanoparticles. Citrate-stabilized AgNPs (Cit-AgNPs) were prepared by the Turkevich method (41). Briefly, 1 mM $AgNO_3$ solution in deionized water was boiled, and sodium citrate solution was added dropwise. The change of color to a grayish yellow indicated the formation of AgNPs. The solution was boiled for an additional 15 min and then cooled to 25°C, followed by dialysis before use for further experiments.

(iii) PVP-capped silver nanoparticles. AgNPs coated with poly(vinylpyrrolidone) (PVP-AgNPs; M_w of 40,000; Fisher Scientific) were prepared as described previously (42). Briefly, 30 ml ethylene glycol was heated at 150°C for 1 h, and 2.5% PVP solution (10 ml in ethylene glycol) was added. Subsequently, 3 mM NaS (0.4 ml in ethylene glycol) and 280 mM AgNO3 (2.5 ml in ethylene glycol) were added. The temperature was maintained at 150°C for 15 min and then allowed to cool to 25°C. Ten milliliters of acetone and 10 ml of Milli-Q water were added, and the mixture was centrifuged at 8,000 × *g*. After four repeated washes, AgNPs were resuspended in deionized water and used for the experiments after dialysis.

AgNP concentrations, zeta potential, and size distribution measurements. AgNP concentrations were measured by using atomic absorption spectrometry (PerkinElmer 2380) with a heated graphite automizer furnace and autosampler AS/71. The sample was analyzed at a 328.1-nm wavelength. For AgNPs, the limit of detection was 0.1 μg/ml. The standard curve was obtained using commercial AgNPs with sizes of 60 nm and 100 nm (Sigma-Aldrich). The particle size distribution and zeta potential were measured by using a Zetasizer Nano ZS apparatus (Malvern, Southborough, MA). In order to measure the charges of the AgNPs, the zeta potential was measured after dialysis.

Bacterial strains used in this study. *Salmonella enterica* serovar Typhimurium (ATCC 14028), *Salmonella enteria* serovar Typhi strain Ty2 (ATCC 700931D), *Shigella flexneri* (MTCC 1457), *Listeria monocytogenes* (MTCC 839), and *Staphylococcus aureus* (ATCC 25923) were used in this study. *S.* Typhimuruym, *S.* Typhi, *S. flexneri*, and *S. aureus* were grown in Luria-Bertani (LB) broth, and *L. monocytogenes* was grown in brain heart infusion (BHI) broth at 37°C with aeration.

Determinations of MICs and MBCs. MICs of different AgNPs were determined by using the broth microdilution method with different bacteria (43, 44). Initially, geometric dilutions (96, 48, 24, 12, 6, 3, 1.5, 0.75, and 0.37 μg/ml) were used, and subsequently arithmetic dilutions (1 to 12 μg/ml) were used to narrow down the differences in MIC values. Aliquots of 100 μl of serially diluted AgNPs in deionized water were added to 100 μl of suspension containing 1×10^5 bacteria in defined 2× M9 medium in 96-well plates ($n = 6$) (44). The plates were incubated at 37°C for 24 h, and the lowest concentration showing no visible growth was recorded as the MIC. From the clear wells, 100 μl of each sample was subcultured to 1 ml of fresh medium, incubated at 37°C for 12 h, and plated in LB agar to determine the minimum bactericidal concentration (MBC).

Antibacterial activities of silver nanoparticles. MICs of different AgNPs were added to 1×10^8 bacteria in 5 ml of phosphate-buffered saline (PBS) and incubated for 2 h with shaking at 37°C. After the incubation, the cultures were serially diluted and plated to check the antibacterial activities of the AgNPs.

Growth curve of *Salmonella* Typhimurium in the presence of silver nanoparticles. *S.* Typhimurium at stationary phase was inoculated into different media (LB, M9 medium, and RPMI 1640 medium [Sigma]) at a 1:100 dilution (5×10^7 bacteria in 5 ml). MICs of AgNPs was added to the media, and the growth of bacteria was evaluated by measuring the optical density (OD) at 600 nm at different time points. RPMI was used as a model for a defined medium without any proteins as the nutrient source.

Silver nanoparticle activity in the presence of blood, serum, plasma, and BSA. A total of 1×10^8 *S.* Typhimurium or *S.* Typhi cells were incubated with MICs of different AgNPs for 2 h in blood, serum, plasma (mouse and human), or 3% bovine serum albumin (BSA) in PBS, plated in LB agar, and incubated at 37°C to check the antibacterial activities of the AgNPs in the presence of these compounds. In the case of blood, EDTA-coated microcentrifuge tubes were used to avoid coagulation.

Silver nanoparticle interactions with BSA. Uncap-AgNPs, Cit-AgNPs, and PVP-AgNPs (10 μg/ml) were incubated with different concentrations of BSA (0.5 to 3.0%) in deionized water at room temperature for 1 h, and the absorption spectrum (300 to 600 nm) was measured using a UV-Vis spectrophotometer (Optizen-3220UV; Daejeon, South Korea). The solution was made such that the AgNP concentration was the same under all conditions. To determine the binding parameters, uncap-AgNPs, Cit-AgNPs, and PVP-AgNPs (10 μg/ml) were incubated with different concentrations of BSA (0 to 10.0%) in deionized water at room temperature for 2 h in 96-well plates. Briefly, 96-well plates were first coated with different concentrations of BSA, and the binding of BSA to the wells was confirmed by estimating the protein concentrations (Bradford method) in the wells after washing. After incubation with different AgNPs, the supernatants were collected to measure the concentration of unbound AgNPs by using an atomic absorption spectrophotometer.

Scanning electron microscopy. *S.* Typhimurium (1×10^8 bacteria/ml) was incubated with different AgNPs (at their MICs) in the presence and absence of 3% BSA for 2 h. After the treatment, bacteria were fixed with glutaraldehyde and dehydrated with increasing concentrations of ethanol for 2 min each. The samples were then stored under vacuum until use. Prior to analysis by field emission-SEM (FEI-Sirion, Eindhoven, Netherlands), the samples were subjected to gold sputtering (JEOL JFC 1100E ion sputtering device).

Flow cytometric analysis. Changes in the membrane potential of *S.* Typhimurium in the presence of AgNPs were assessed by using the membrane potential-sensitive dye bis-(1,3-dibutylbarbituric acid) trimethine oxonol [$DiBAC_4(3)$] as described elsewhere (45). Briefly, logarithmic-phase *S.* Typhimurium (10^7 CFU/ml) cells were incubated with different AgNPs (at the corresponding MICs) in the presence and absence of 3% BSA at 37°C for 2 h. Cells were collected by centrifugation (6,000 × *g* for 10 min), 500 μl $DiBAC_4(3)$ (1 μg/ml) was added, and the mixture was incubated at 25°C for 5 min in the dark. The cells were washed and subjected to flow cytometric analysis (BD FACSCanto II), and the data were analyzed with WinMDI 2.9.

MTT assay. The *in vitro* cytotoxicities of different AgNPs were assessed using a 3-(4,5-dimethyl-2-thiazolyl)-2,5-diphenyl-2H-tetrazolium bromide (MTT) assay in RAW 264.7 and intestine 407 cell lines (kind gifts of M. S. Patole, National Center for Cell Science, Pune, India, and Syamal Roy, IICB, Kolkatta, India). All cell lines were maintained in Dulbecco's modified Eagle's medium (DMEM; Sigma) supplemented with 10% fetal calf serum (Sigma) at 37°C and 5% CO_2. Cells were counted with a hemocytometer, and 5×10^4 cells were seeded in 96-well plates and incubated for 8 h. The cells were incubated with various concentrations of AgNPs in the presence and absence of serum (10%) for 24 h. After incubation and washes with PBS, 20 μl of MTT dye (5 mg/ml) was added to each well, and the mixtures were kept for 4 h at 37°C. The percentage of cell viability was determined at 570 nm and is reported relative to that for cells that were not treated with AgNPs (46).

Trypan blue exclusion assay. A trypan blue exclusion assay (47) was performed to check the cytotoxicity of different AgNPs for RAW 264.7 and intestine 407 cell lines. A total of 1×10^5 cells were seeded in a 24-well plate. The cells were incubated with 10 μg/ml and 50 μg/ml of AgNPs in the presence and absence of serum (10%) for 24 h in DMEM. The cells were trypsinized and centrifuged for 5 min at 100 × *g*. The cell pellet was resuspended in 1 ml of PBS, and 10 μl of cell suspension was mixed with 10 μl of 0.4% trypan blue and incubated for 3 min at room temperature. The number of dye-excluding cells was counted by using a hemocytometer. A minimum of 200 cells were counted, and the percent viability was calculated in comparison to the control.

Intracellular concentrations of AgNPs. Uncap-AgNPs, Cit-AgNPs, and PVP-AgNPs (10 μg/ml) were incubated with RAW 264.7 and intestine 407 cell lines for 2 h in DMEM (without serum) in the presence and absence of 3% BSA. After incubation, the supernatant was collected to measure the extracellular AgNP concentration. The extracellular medium was centrifuged at 50,000 × *g*, and the AgNPs were resuspended in deionized water. The AgNP concentration (in extracellular medium) was determined by atomic absorption spectrophotometer as described earlier. The internal concentration and percent uptake were calculated by subtracting the concentration of input AgNPs from the remaining AgNPs in the extracellular medium.

Gentamicin protection assay. For the gentamicin protection assay, cells were counted with a hemocytometer, and 1×10^5 cells (RAW 264.7 or intestine 407) were seeded per well in a 24-well plate and incubated for 8 h. The *S.* Typhimurium strain was grown to stationary phase in LB for the infection of RAW 264.7 cells. Stationary-phase cultures (*S.* Typhimurium and *S.* Typhi) were diluted 1:33 in LB and grown for 3 h (late exponential phase) for infection of epithelial cells (intestine 407). This was done to induce the SPI-1 genes required for invasion of nonphagocytic cells (29). The gentamicin protection assay was performed as described previously (48). Briefly, RAW 264.7 and intestine 407 cells were infected with *Salmonella* (multiplicity of infection [MOI], 10) and incubated for 30 min, after which the data time points began. After repeated washes with PBS, DMEM containing gentamicin (100 μg/ml) was added, and cells were incubated for 1 h to kill all extracellular bacteria. Then, different AgNPs were added (10 μg/ml) and incubated for 1 h in DMEM (with or without serum/BSA) that contained gentamicin (25 μg/ml). At 2 h and 16 h, cells were lysed with 0.1% Triton X-100 and plated on LB agar for bacterial counts. The change in intracellular replication was calculated by dividing the intracellular bacterial load at 16 h by the bacterial load at 2 h.

***In vivo* experiment.** BALB/c mice were bred and housed at the Central Animal Facility at the Indian Institute of Science. The mice used for the experiments were 6 to 8 weeks old. All procedures with animals were carried out in accordance with the institution ethics for animal handling. Mice were infected with *S.* Typhimurium orally (1×10^7 CFU/mouse; 5 mice in each group). Single doses of different AgNPs and a PBS control were administered orally (100 mg/kg of body weight) or intravenously (i.v.; 20 mg/kg) daily for 3 days. Ciprofloxacin (10 mg/kg) was used as the positive control. The mice were sacrificed after 4 days, and the liver, spleen, and mesenteric lymph nodes (MLN) were aseptically isolated, weighed, and homogenized in sterile PBS. The homogenate was plated in serial dilutions on salmonella-shigella (SS) agar to determine the bacterial load in various organs. The CFU was determined, and results are presented as the CFU per gram of organ.

Survival assay. Cohorts of mice (8 per group) were treated with different AgNPs or ciprofloxacin (10 mg/kg) orally or intravenously for 4 days after *S.* Typhimurium infection (10^8 CFU/mouse [oral administration group]). The animals were checked for morbidity and mortality twice daily for 15 days.

Statistical analysis. For analyzing data, the data were subjected to statistical analysis by applying Student's *t* test, the Mann-Whitney U test, and log rank test by using commercially available GraphPad Prism 5 software. A *P* value of <0.05 was considered significant.

RESULTS

The antibacterial activities of AgNPs are strongly dependent on the capping of AgNPs. The antibacterial properties of AgNPs are used in medical applications to avoid microbial infections. Initially, we synthesized AgNPs by the chemical reduction method, and uncap-AgNPs did not show any antibacterial effect against *Salmonella* when tested in LB broth (data not shown). However, efficient killing of bacteria was observed when PBS was used instead of LB broth (Fig. 1A). Since the antibacterial property of AgNPs is crucial for many applications in the medical field, we further synthesized different AgNPs to understand the underlying mechanism. In the study, we synthesized 3 different types of AgNPs, namely, uncap-AgNPs by the chemical reduction method, Cit-AgNPs, and PVP-AgNPs. The size distribution of AgNPs was studied by using dynamic light scattering (DLS). The size distributions of uncap-AgNP (75 ± 4.5 nm [mean ± standard deviation, or SD]), Cit-AgNP (82 ± 5.2 nm), and PVP-AgNP (86 ± 6.7 nm) showed comparable size ranges. The antibacterial properties of these nanoparticles against different Gram-negative and Gram-positive bacteria were analyzed. The Cit-AgNPs and PVP-AgNPs were found to exhibit the antibacterial property in LB broth, which might be due to either prevention of interaction of AgNPs via components of LB or prevention of agglomeration of these particles. Subsequently, experiments were carried out to understand the mechanism behind the aforementioned observation. MICs and MBCs of these different nanoparticles were established against Gram-negative (*S.* Typhimurium, *S.* Typhi, and *Shigella*) as well as Gram-positive (*Listeria monocytogenes* and *S. aureus*) bacteria (Tables 1 and 2). The MICs of different AgNPs ranged from 6 to 8 μg/ml. An earlier report suggested that AgNPs of 70

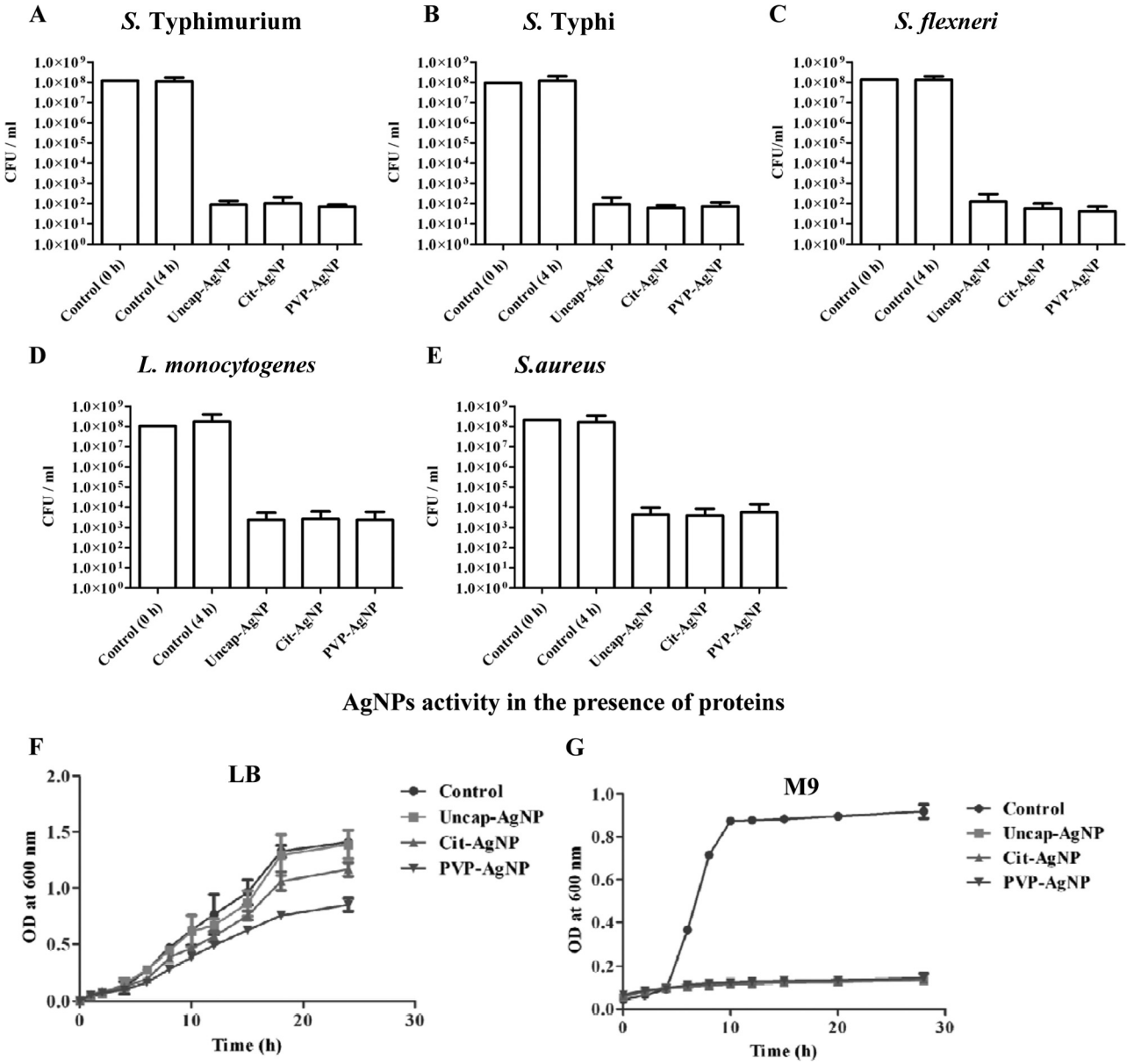

FIG 1 Antimicrobial activity of AgNPs. The antimicrobial activities of uncap-AgNPs, Cit-AgNPs, and PVP-AgNPs against different Gram-negative [*S.* Typhimurium (A), *S.* Typhi (B), and *S. flexneri* (C)] and Gram-positive [*L. monocytogenes* (D) and *S. aureus* (E)] species were tested in PBS with AgNPs (based on the MICs). The growth curve for *S.* Typhimurium was established in LB (F) and M9 medium (G) by subculturing overnight LB broth-grown cells at 1:100 in the respective medium.

nm to 100 nm exhibit similar MICs against different bacteria (49). The MICs of different AgNPs were used for other *in vitro* experiments. Initially, the antibacterial properties of AgNPs were assessed in different pathogens, and we used *S.* Typhimurum as a model system to verify the role of capping agents in the AgNPs antibacterial property.

When different AgNPs were incubated with 10^8 bacteria/ml for 2 h in PBS, the AgNPs were able to kill the bacteria. All the AgNPs

TABLE 1 MICs of different silver nanoparticle preparations

AgNPs preparation	MIC[a] (μg/ml)				
	S. Typhimurium	*S.* Typhi	*S. flexneri*	*L. monocytogenes*	*S. aureus*
Uncap-AgNP	6.00 ± 0.50	6.33 ± 0.29	7.00 ± 0.50	7.33 ± 0.29	7.33 ± 0.29
Cit-AgNP	6.33 ± 0.76	6.33 ± 0.58	6.67 ± 0.29	7.50 ± 0.50	7.67 ± 0.58
PVP-AgNP	6.33 ± 1.04	6.83 ± 0.29	6.67 ± 0.58	7.67 ± 0.58	7.83 ± 0.76

[a] Data (means ± SD) were obtained from geometric dilutions of different AgNPs.

TABLE 2 MBCs of different silver nanoparticle preparations

AgNPs preparation	MBC[a](μg/ml)				
	S. Typhimurium	*S.* Typhi	*S. flexneri*	*L. monocytogenes*	*S. aureus*
Uncap-AgNP	7.17 ± 0.29	7.67 ± 0.29	8.00 ± 0.50	9.17 ± 0.29	8.83 ± 0.76
Cit-AgNP	7.17 ± 0.76	7.83 ± 0.76	8.17 ± 0.29	8.83 ± 0.76	9.00 ± 0.50
PVP-AgNP	7.67 ± 0.58	7.50 ± 0.50	8.17 ± 0.58	9.33 ± 0.29	8.83 ± 0.29

[a] Data (means ± SD) were obtained from geometric dilutions of different AgNPs.

showed similar antibacterial effects when they were incubated with bacteria in PBS (Fig. 1A to E). When these AgNPs were incubated with *S.* Typhimurium in LB broth and checked for growth, significant differences were observed between the different AgNPs (Fig. 1F). There was no increase in the OD at 600 nm when different AgNPs were added to M9 minimal medium (without proteins) (Fig. 1G). A similar result was observed when RPMI medium (without serum) was used for the growth of *S.* Typhimurium (see Fig. S1A in the supplemental material).

Biological fluids, like blood, serum, and plasma, completely inhibited the antibacterial activity of uncapped AgNPs. With the emergence of multidrug resistance, treatment for bacterial infections has become very challenging (50–53). Interest has been generated for AgNPs because of their excellent antimicrobial properties (39, 54). AgNPs have also shown antiviral properties (55). There are very few reports suggesting resistance development in bacteria against silver (18, 56). We exploited a salmonellosis model to study the antibacterial properties of different AgNPs under *in vitro* and *in vivo* conditions. To test the effect of AgNPs under *in vivo* conditions, different AgNPs were added to whole blood, serum, or plasma and then incubated either with *S.* Typhimurium or *S.* Typhi. In the absence of serum, blood, or plasma, there was no significant difference in the antibacterial activity of different types of AgNPs. However, serum, blood, and plasma each inhibited the activity of uncap-AgNPs completely, but not Cit-AgNPs or PVP-AgNPs. Under all the conditions tested, the activity of PVP-AgNPs was better than that of Cit-AgNPs (Fig. 2A and B). Antibacterial activity toward *S.* Typhimurium was analyzed in the presence of mouse blood, serum, and plasma, whereas for *S.* Typhi the antibacterial activity was analyzed in the presence of human blood components (Fig. 2B; see also Fig. S1B in the supplemental material). Since serum albumin is the major component of blood, 3% BSA was further used to assess the antibacterial effects of different AgNPs. Addition of BSA totally abrogated the antibacterial activity of uncap-AgNPs, but not that of capped AgNPs (Fig. 2C).

BSA exhibited a different interaction pattern with capped versus uncap-AgNPs, with resulting differences in killing activity. In our study, PVP-AgNPs showed the least interaction with serum albumin and hence better antibacterial activity in the presence of BSA. To confirm this finding, different AgNPs (at the same concentration) were incubated with 3% BSA, and the absorption spectrum was analyzed (57). The results suggested that uncap-AgNPs have more interaction with BSA, and PVP-AgNPs have the least. Cit-AgNPs showed a moderate interaction with BSA (Fig. 3A to D). The membrane potential-sensitive dye $DiBAC_4(3)$ was used to check the change in membrane potential (45) of *S.* Typhimurium upon incubation with different AgNPs in the presence and absence of 3% BSA. Flow cytometric analysis clearly showed that, in the absence of BSA, there was no difference in the change in the membrane poteintial of bacteria for any of the AgNPs, whereas in the presence of BSA, no membrane damage was observed in the case of uncap-AgNPs, and the extent of damage was high when PVP-AgNPs were used. Moderate damage was observed when *S.* Typhimurium was incubated with Cit-AgNPs (Fig. 3E; see also Fig. S2 in the supplemental material). For further confirmation, *S.* Typhimurium incubated with different AgNPs in the presence and absence of BSA was analyzed via scanning electron microscopy (SEM). SEM images clearly showed that damage when *S.* Typhimurium was treated with all the different AgNPs in the absence of BSA, but in the presence of BSA, only PVP-AgNPs caused damage to the bacteria (see Fig. S3 in the supplemental material). When different AgNPs were incubated with different concentrations of BSA, most of the uncap-AgNPs were bound to BSA (present at 4%), whereas binding was not observed with PVP-AgNPs, and moderate binding was observed with Cit-AgNPs (Fig. 3F).

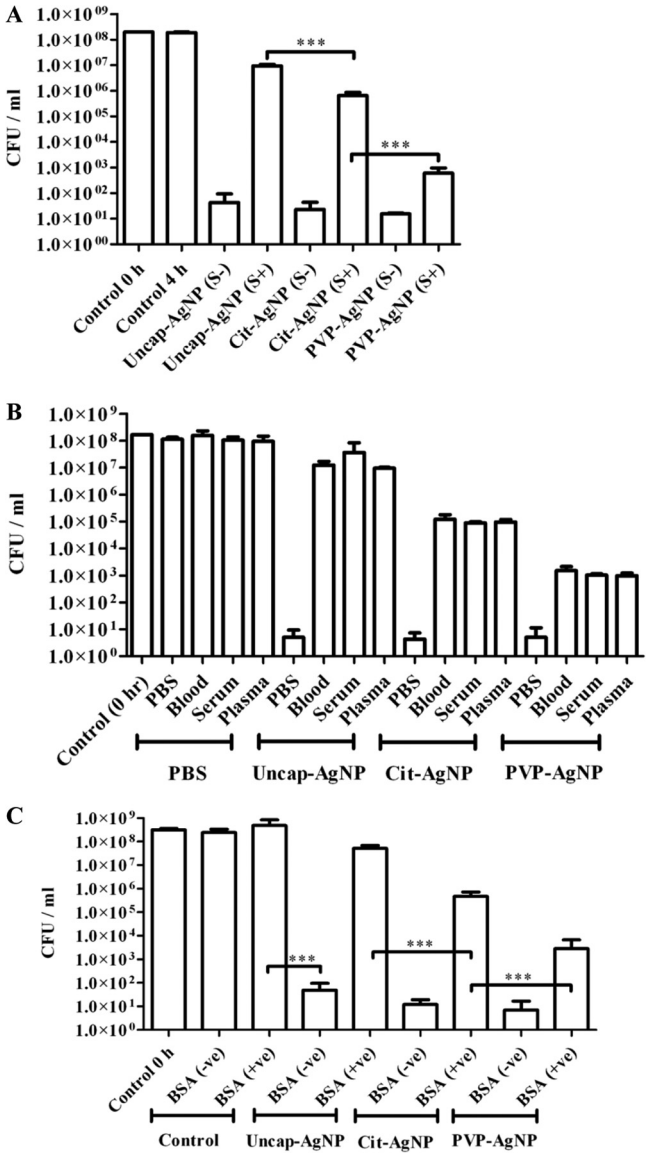

FIG 2 AgNP activities in the presence of blood, serum, plasma, and BSA. The antibacterial effects of different AgNPs for *S.* Typhimurium were tested in the presence of bovine serum (A), mouse blood, serum, and plasma (B), and 3% bovine serum albumin (C). Values that are significantly different by Student's *t* test are indicated by a bracket with asterisks, as follows: ***, $P < 0.0005$.

***In vitro* cell culture models demonstrated the similar pattern of killing by uncapped and capped AgNPs, as shown in the broth.** To investigate the killing patterns further, we used an *in vitro* cell culture model for *Salmonella* infection. *Salmonella* infects epithelial cells and macrophages of various organs. The activities of different AgNPs against *Salmonella* were investigated in the presence and absence of serum in epithelial cells (intestine 407) and macrophages (RAW 264.7). A trypan blue exclusion as-

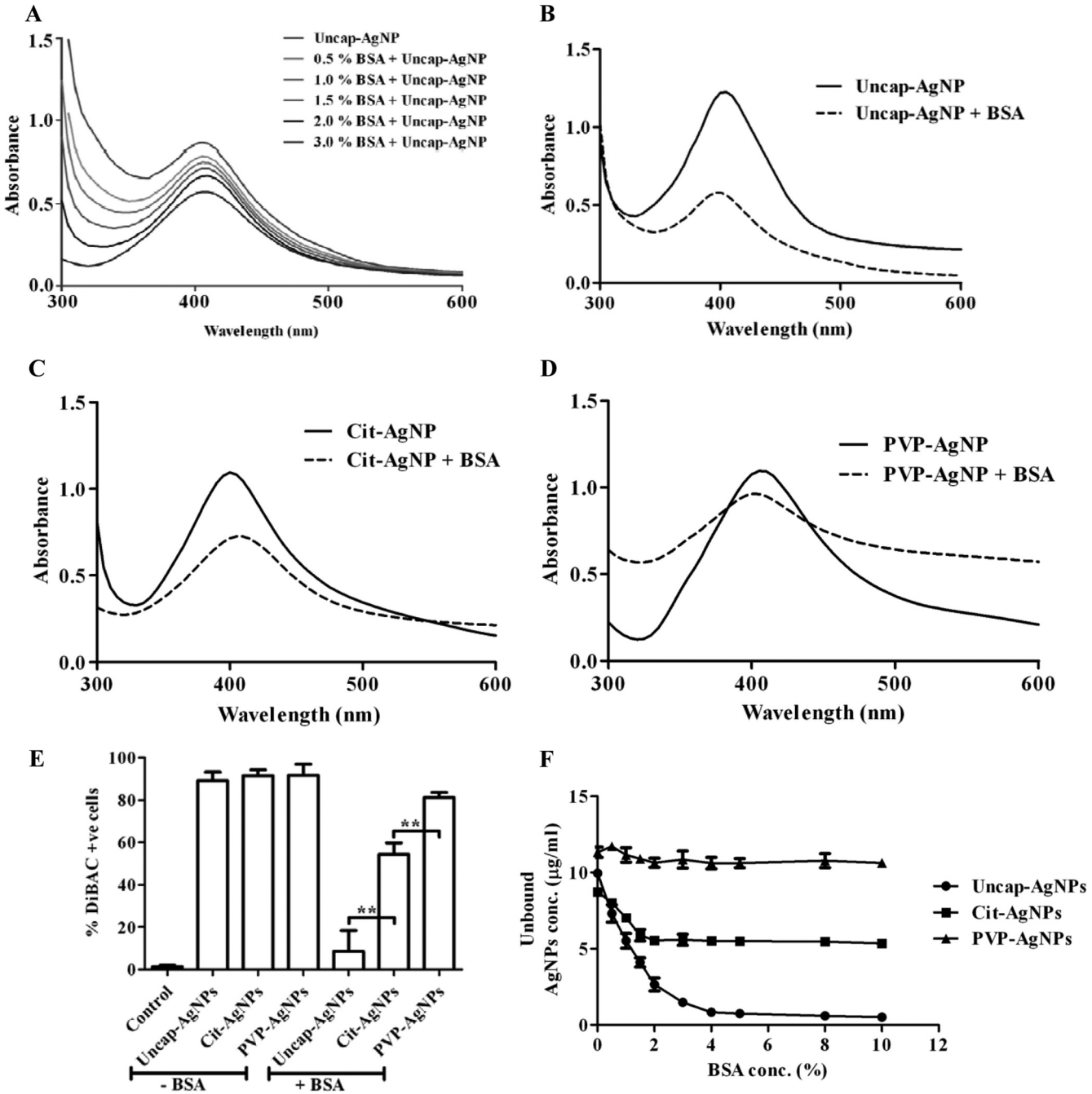

FIG 3 AgNP interactions with BSA. (A) Uncap-AgNPs were incubated with different concentrations of BSA, and the absorbance spectrum was checked. (B to D) The absorbance spectra of uncap-AgNP (B), Cit-AgNP (C), and PVP-AgNP (D) were obtained by incubating these NPs with 3% BSA. (E) The change in the bacterial membrane potential of *S.* Typhimurium (STM) was analyzed by flow cytometry by using $DiBAC_4(3)$. *S.* Typhimurium was incubated with different AgNPs in the presence and absence of 3% BSA, and DiBAC-positive cells were quantitated by flow cytometry. Flow cytometric data were analyzed with WinMDI 2.9. Values that are significantly different by Student's *t* test are indicated by brackets with asterisks as follows: **, $P < 0.005$. (F) Uncap-AgNPs, Cit-AgNPs, and PVP-AgNPs (10 μg/ml) were incubated with different concentrations of BSA (0 to 10.0%) in deionized water at room temperature for 2 h in 96-well plates, and the unbound AgNPs concentration was determined by atomic absorption spectrophotometry.

say and an MTT uptake assay were performed to estimate the viability of these cells in the presence of different AgNPs. AgNPs at 10 μg/ml did not show any toxic effect on the different cell lines, whereas concentrations of 20 μg/ml and above created significant toxicity to these cells in the absence of serum. Although the MTT assay showed that there was no difference in the viability in the presence of serum for Cit-AgNPs and PVP-AgNPs, the trypan blue exclusion assay revealed that indeed there was a significant reduction in the viability of the cells when capped AgNPs were used in the presence of serum (see Fig. S4A and B and 5A and B in the supplemental material). In the presence of serum, uncap-AgNPs did not affect the viability of the cells at the 50 μg/ml

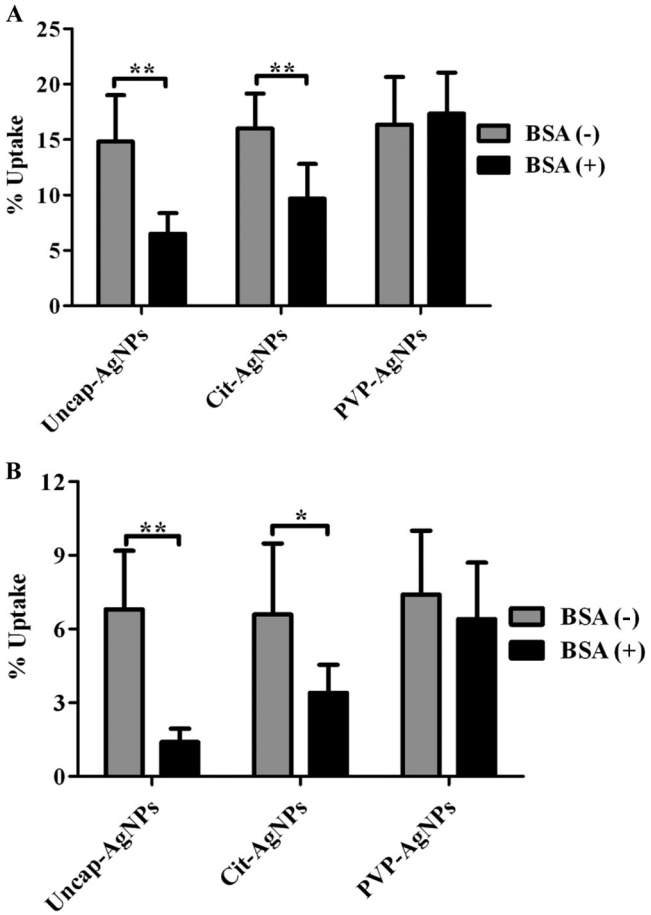

FIG 4 AgNP uptake studies. The graphs show the different AgNP uptake percentages by RAW 264.7 (A) and intestine 407 (B) cell lines in the presence and absence of 3% BSA. Cells were incubated with different AgNPs in the presence (BSA+) and absence (BSA-) of 3% BSA for 2 h, and the intracellular concentrations of AgNPs were determined by measuring the extracellular AgNP concentration in the medium via atomic absorption spectrometry. Values that are significantly different by Student's *t* test are indicated by brackets with asterisks as follows: *, $P < 0.05$; **, $P < 0.005$.

concentration, whereas Cit-AgNPs and PVP-AgNPs created significant toxicity for the cells at the same concentration. This may have been due to the interaction of the uncap-AgNPs with serum proteins. Intracellular concentrations of AgNPs were measured to determine the cellular uptake by these cells. There was no significant difference in the uptake of different AgNPs in the absence of BSA, whereas the uptake of uncap-AgNPs was significantly lower in the presence of BSA with these cell lines (Fig. 4A and B). There was no significant difference in the uptake when PVP-AgNPs were used in the presence of 3% BSA. The gentamicin protection assay was carried out to check the antibacterial activity of different AgNPs inside the cells. *S.* Typhimurium-infected RAW 264.7 and intestine 407 cells were treated with different AgNPs, and their intracellular growth was determined. In the absence of serum, AgNPs killed the intracellular bacteria, whereas the presence of serum completely inhibited the activity of uncap-AgNPs but not of capped AgNPs (Fig. 5A and B). Similar results were obtained when 3% BSA was used instead of serum (Fig. 5C and D). These results clearly indicated that the presence of BSA inhibits the uptake of the AgNPs and, hence, the difference in the antibacterial activities of these particles was observed *in vitro*.

The *in vivo* mouse model of systemic typhoid fever strongly suggested the importance of AgNP preparations for therapeutic use. A murine salmonellosis model, which is an excellent *in vivo* model for systemic infection by *Salmonella*, was used to understand the differential effect of AgNPs in the presence and absence of capping agents. BALB/c mice were infected with *S.* Typhimurium (10^7 CFU, orally), treated with different AgNPs for 3 days, and the bacterial burdens in MLN, spleen, and liver were analyzed. Different AgNPs were administered orally as well as i.v. to treat *Salmonella* infection in mice. No effect of AgNPs was observed when uncap-AgNPs were administered to treat *Salmonella* infection, whereas the capped AgNPs were able to reduce the bacterial burden in different organs (Fig. 6A and B). Most importantly, with the *in vivo* mouse model of infection, PVP-AgNPs showed a greater antibacterial effect.

Finally, we confirmed the role of capping agents for their antibacterial activity by treating the mice with different AgNPs (oral and i.v.) after infection with *S.* Typhimurium. Mice were infected with a lethal dose of *S.* Typhimurium (10^8 CFU) and treated with different AgNPs and ciprofloxacin. While all the mice recovered from *Salmonella* infection when treated with ciprofloxacin, AgNPs could not protect the mice completely from *Salmonella* infection. When uncap-AgNPs were used, all the mice died, after the same duration as in controls, whereas Cit-AgNPs and PVP-AgNPs delayed the deaths of the mice. When different AgNPs were administered intravenously, PVP-AgNPs protected 60% of the mice from death (Fig. 7A and B).

DISCUSSION

Studies have been carried out on different microorganisms selected from the ATCC strain collection to prove the antibacterial property of AgNPs (3). However, there have been doubts regarding the efficacy of AgNPs against bacterial clinical isolates, owing to antibiotic resistance. Further studies have proved that the AgNPs are equally effective against clinical isolates such as *E. coli*, *E. faecalis*, *P. aeruginosa*, *S. aureus*, and *Stenotrophomonas maltophilia* (58). Studies have also proved that the smaller the size of zinc oxide particles, the greater the efficacy in inhibiting the growth of bacteria, based on both the production of reactive oxygen species and accumulation of nanoparticles (59). Selenium nanoparticles have been found to inhibit the growth of *S. aureus*, similarly to iron oxide with polyvinyl alcohol (60, 61). Similarly, glycan-encapsulated gold nanoparticles selectively inhibit Shiga toxins 1 and 2 (62). Our study found that uncap-AgNPs had antibacterial properties against *Salmonella* in PBS but not in LB broth. This loss of antibacterial activity in the presence of LB broth may be due to the interaction of AgNPs with proteins that are present in the medium (57, 63). It was also conclusively proved that all three types of nanoparticles, i.e., uncap-AgNPs, Cit-AgNPs, and PVP-AgNPs, are equally proficient for their antibacterial properties in PBS. In the absence of proteins, as in PBS, all three AgNPs showed similar antibacterial properties. However, in LB broth, the capping of AgNPs played an important role in determining the antibacterial effect. It has been reported that capping agents can stabilize the AgNPs by avoiding the aggregation of the particle as well as providing protection from temperature and light (12–14, 64). Enhanced antibacterial activity was also observed when AgNPs were coated with different capping agents

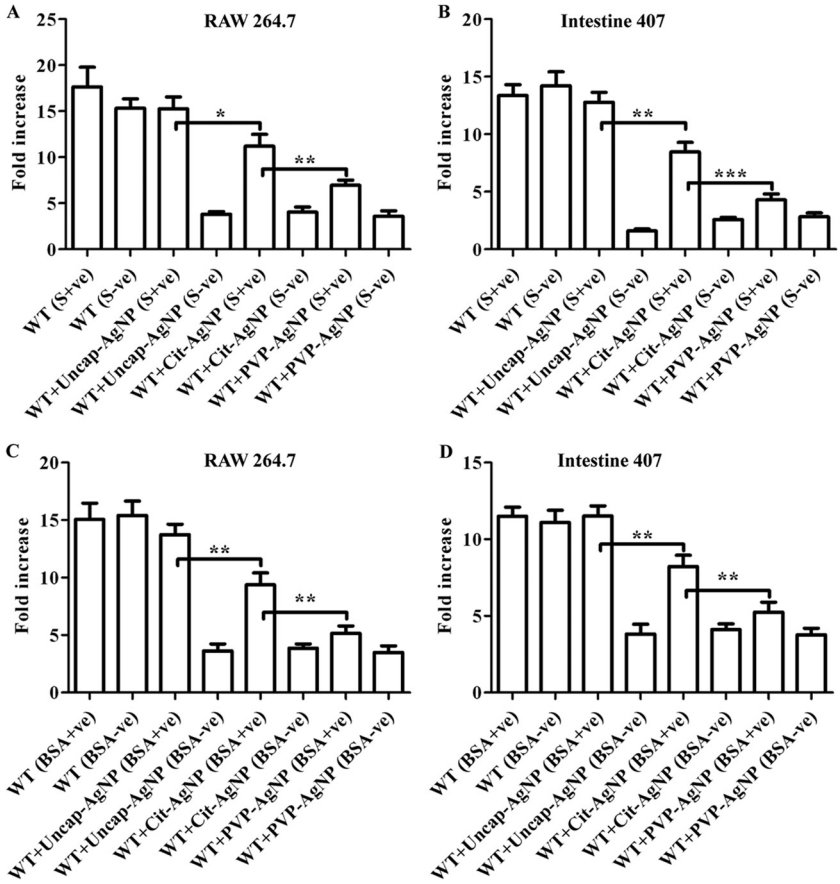

FIG 5 *In vitro* activities of AgNPs. Stationary-phase and late-log-phase *S.* Typhimurium cells were used to infect RAW 264.7 (A and C) and intestine 407 (B and D) cells, respectively, at an MOI of 10. Different AgNPs (10 μg/ml) were added in the presence and absence of 10% serum (A and B) and 3% BSA (C and D). The fold increase in the bacterial count was determined by plating extracts 2 h and 16 h after lysing the cells. Values that are significantly different by Student's *t* test are indicated by a bracket and asterisks as follows: *, $P < 0.05$; **, $P < 0.005$; ***, $P < 0.0005$.

(12–14). We wanted to elucidate the antibacterial role of capping agents apart from providing stabilization to the AgNPs.

Numerous studies on the interaction of NPs with blood, serum, and other proteins have thrown light on the unique properties that we have discussed here. Gold NPs that interacted with BSA in aqueous solution led to a red shift of the plasmon resonance maximum by 5 to 6 nm. These results could be used for studying optical and physicochemical properties of NPs *in vivo* and mechanisms of the interaction of NPs of noble metals with biological objects (65). Interactions of AgNPs with BSA were found to be spontaneous and driven by hydrophobic forces with changes in the microenvironment of the tryptophan residues along with dynamic and static quenching of the BSA fluorescence (63). Another study showed that the BSA adsorption on the surface of AgNPs effectively prevented aggregation and flocculation, thereby enhancing the uptake of the NPs into live cells (57). With cases such as magnetic iron oxide NPs, the secondary structure of BSA molecules has been found to change drastically (66). As the size of gold NPs was increased, enhanced protein packing in the larger NPs and effective screening of the charge interaction between the NPs were observed (67).

Protein adsorption onto nanoparticles occurs due to an increase in the collective entropy of the proteins on the NP surface and nonspecific interactions between the NP surface and the proteins. The increase in the entropy is due to the rearrangement of the protein structure to a more stable position on the uncoated AgNP surface. Strong interactions occur between uncoated AgNPs and proteins due to the increase in entropy, which in turn leads to a significant decrease in the Gibbs free energy. This decrease in energy is primarily due to the relaxation of protein secondary structures (68). Cellular uptake of different AgNPs is found to be modulated by their interactions with different components of blood, including albumin, transferrin, and IgG (69).

All the studies that have been carried out to date have shown that the antimicrobial activities of the NPs diminished upon interaction with serum proteins. However, our study conclusively proved that coating the AgNPs with citrate or PVP effectively maintained the antibacterial property both in the *in vitro* cell culture model as well in the *in vivo* animal model. The toxicities of these AgNPs to mammalian cells were altered in the presence of serum. There was no significant difference in the viability of the cells for Cit-AgNPs and PVP-AgNPs in the presence of serum (see Fig. S5A and B in the supplemental material). The difference in the viability of the mammalian cells in the presence of serum with different AgNPs was not revealed in the MTT assay. However, a trypan blue exclusion assay showed that there was a significant reduction in the viability of the cells when Cit-AgNPs or PVP-AgNPs were used in the presence of serum (see Fig. S4A and B in

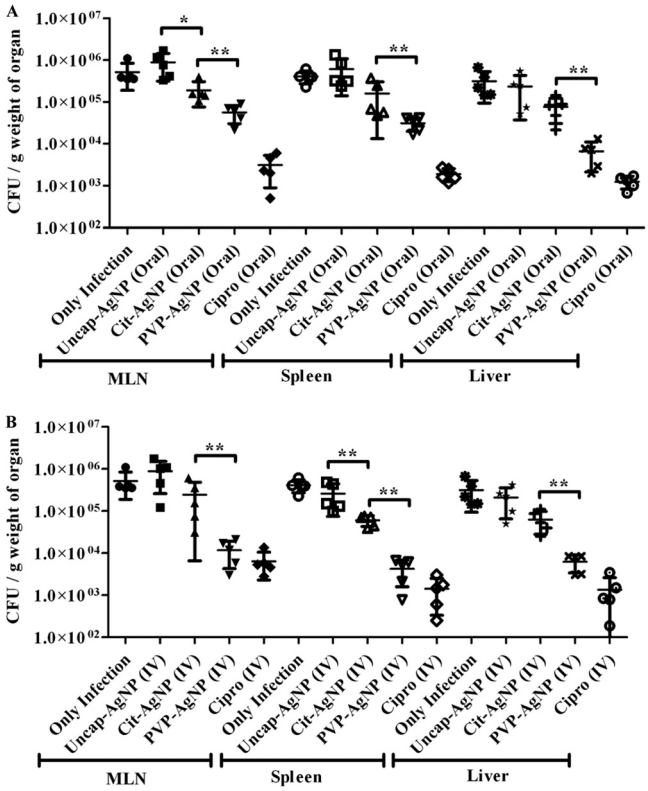

FIG 6 *In vivo* activitues of AgNPs based on the *Salmonella* burden in different organs. BALB/c mice were infected with *S.* Typhimurium (1×10^7 CFU) and then treated with different AgNPs and ciprofloxacin (10 mg/kg). AgNPs were administered by the oral route (100 mg/kg of body weight) (A) or the intravenous route (20 mg/kg of body weight) for 3 days (B), and the bacterial burdens in different organs (MLN, spleen, and liver) were determined on the fifth day after infection. The organs were collected aseptically, and the tissues were homogenized and plated on SS agar and incubated at 37°C. Values that are statistically different by the Mann-Whitney U test are indicated by a bracket and asterisks as follows: *, $P < 0.05$; **, $P < 0.005$.

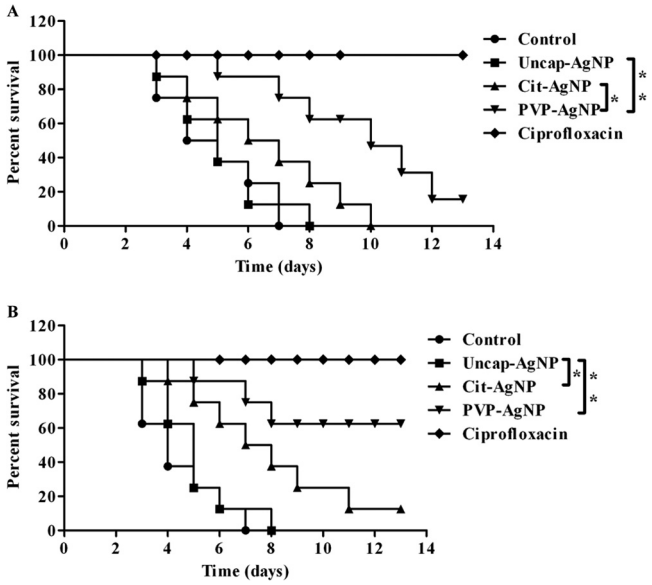

FIG 7 *In vivo* activities of AgNPs, determined in a survival assay. BALB/c mice were infected with a lethal dose of *S.* Typhimurium (10^8 CFU) and then treated with different AgNPs and ciprofloxacin (20 mg/kg) for 4 days. AgNPs were given by the oral route (100 mg/kg of body weight) (A) or the intravenous route (20 mg/kg of body weight) (B), and then mice were assessed for morbidity and mortality twice daily for 15 days. Values that are statistically different by the log rank test are indicated by a bracket and asterisks as follows: *, $P < 0.05$; **, $P < 0.005$.

the supplemental material). This may have been due to the fact that the trypan blue exclusion assay examines the membrane integrity of cells, whereas the MTT assay examines the metabolic activity of the cells. Serum albumin in the blood was found to have a differential interaction with different AgNPs, and hence the antibacterial effects of AgNPs can be altered. All the AgNPs showed saturation in the binding with BSA at a 3 to 4% concentration. The binding of PVP-AgNPs to BSA was very minimal, whereas maximum binding was observed for uncap-AgNPs. These results indicate that the interaction of AgNPs with BSA is altered when different capping agents are used. The interaction of uncapped AgNPs with serum proteins may be the reason for the lack of antibacterial activity *in vivo*. Previously, the effects of different AgNPs and their roles in antibacterial activity were not studied *in vivo*.

Here we have demonstrated for the first time that the synthesis methods and the capping agents employed play crucial roles for the antibacterial activity of AgNPs in the *in vivo* model system. The synthesis methods and capping agents can be optimized to gain better antibacterial as well as antiviral activities *in vivo*.

With reference to the *in vivo* models, a study has been carried out in a chick model with AgNPs in combination with nanosilicate platelets (NSP). It was observed that AgNP/NSP effectively controlled enteric *Salmonella* infection. In addition, when amoxicillin was used in conjunction with this combination, only 1/10 of the normal dosage of the drug was required to obtain roughly 80% protection from salmonellosis. The main advantage of such a scenario is that it reduced the emergence of antibiotic-resistant bacteria (38). Gold NPs were found to inhibit VEGF-165 (vascular endothelial growth factor 165)-induced permeability and angiogenesis *in vivo* in the nude mouse ear model (70). A silver carbene complex loaded on L-tyrosine polyphosphate (SCC) NPs and then administered to *Pseudomonas aeruginosa*-infected mice resulted in a 20% survival advantage. Further, in the same study, the lungs from the majority of the mice treated with SCC NPs appeared normal, with a significant decrease in the bacterial burdens in the lungs (71).

Silver nanoparticles may cause side effects due to interactions with proteins in the body, the alpha-beta transition, and protein aggregation (72). In the use of AgNPs to generate better antibacterial properties *in vivo*, the capping agents and synthesis method play crucial roles. We demonstrated the variable action of AgNPs *in vivo* when capped with different capping agents. PVP-AgNPs showed better antibacterial properties *in vitro* as well as *in vivo* compared to Cit-AgNPs. The reason for this may be due to the better stability and higher uptake by the cells with the PVP-AgNPs. The uptake of the capped AgNPs was significantly higher than for uncap-AgNPs in the presence of serum. This better uptake may be the reason for better killing of intracellular *Salmonella*. The reason for better uptake may be due to the fact that the interaction of AgNPs was minimized when capping agents were used. With all these results, we can conclude that the capped AgNPs interaction with BSA is minimal; hence the uptake is higher, and the intracellular killing of bacteria is higher. When

AgNPs were administered intravenously, the mice were found to have higher survival compared to those that received orally administered AgNPs. This could be attributed to the fact that orally administered AgNPs are excreted through feces (38). This study is the first of its kind to throw light on the importance of the capping agent with regard to the antibacterial activity under physiological conditions in an animal model. This study puts forward a note of caution that the efficacy of AgNPs varies between PBS and biological fluids. Hence, all the *in vitro* assays that demonstrated good antibacterial activity for AgNPs should be reassessed in the presence of biological fluids, and preferably in the *in vivo* model systems. Further future avenues can be directed toward formulating new capping agents for AgNPs with the best antibacterial activity, with or without the combinatorial therapy with antibiotics.

ACKNOWLEDGMENTS

We thank Michael Hensel for providing the *Salmonella* strains. We thank Monalisha Elango for assistance in the work. We thank Namrata Iyer and Preeti Garai for critical comments. We thank the Electron Microscopy facility and Flow Cytometry facility for help with these studies. We thank the Central Animal Facility (CAF) for providing the mice.

This work was supported by the grant Provision (2A) Tenth Plan (191/MCB) from the director of the Indian Institute of Science, Bangalore, India, and the Department of Biotechnology (DBT 311, NBA, sanctioned by the President), Life Science Research Board (LSRB0008), and DBT-IISc Partnership Program for Advanced Research in Biological Sciences and Bioengineering to D.C. Infrastructure support from ICMR (Center for Advanced Study in Molecular Medicine), DST (FIST), and UGC (special assistance) is acknowledged. D.P.G. and M.B.T. are research scholars, and R.T. is a project assistant.

REFERENCES

1. **Meng H, Liong M, Xia T, Li Z, Ji Z, Zink JI, Nel AE.** 2010. Engineered design of mesoporous silica nanoparticles to deliver doxorubicin and P-glycoprotein siRNA to overcome drug resistance in a cancer cell line. ACS Nano **4:**4539–4550.
2. **Kohl Y, Kaiser C, Bost W, Stracke F, Fournelle M, Wischke C, Thielecke H, Lendlein A, Kratz K, Lemor R.** 2011. Preparation and biological evaluation of multifunctional PLGA-nanoparticles designed for photoacoustic imaging. Nanomedicine **7:**228–237.
3. **Rangari VK, Mohammad GM, Jeelani S, Hundley A, Vig K, Singh SR, Pillai S.** 2010. Synthesis of Ag/CNT hybrid nanoparticles and fabrication of their nylon-6 polymer nanocomposite fibers for antimicrobial applications. Nanotechnology **21:**095102. doi:10.1088/0957-4474/21/9/095102.
4. **Lok CN, Ho CM, Chen R, He QY, Yu WY, Sun H, Tam PK, Chiu JF, Che CM.** 2007. Silver nanoparticles: partial oxidation and antibacterial activities. J. Biol. Inorg. Chem. **12:**527–534.
5. **Morones JR, Elechiguerra JL, Camacho A, Holt K, Kouri JB, Ramirez JT, Yacaman MJ.** 2005. The bactericidal effect of silver nanoparticles. Nanotechnology **16:**2346–2353.
6. **Rai M, Yadav A, Gade A.** 2009. Silver nanoparticles as a new generation of antimicrobials. Biotechnol. Adv. **27:**76–83.
7. **Lee J-M, Kim D-W, Kim T-H, Oh S-G.** 2007. Facile route for preparation of silica-silver heterogeneous nanocomposite particles using alcohol reduction method. Mater. Lett. **61:**1558–1562.
8. **Quang DV, Sarawade PB, Hilonga A, Park SD, Kim J-K, Kim HT.** 2011. Facile route for preparation of silver nanoparticle-coated precipitated silica. Appl. Surf. Sci. **257:**4250–4256.
9. **Park J-H, Park J-K, Shin H-Y.** 2007. The preparation of Ag/mesoporous silica by direct silver reduction and Ag/functionalized mesoporous silica by in situ formation of adsorbed silver. Mater. Lett. **61:**156–159.
10. **Sharma VK, Yngard RA, Lin Y.** 2009. Silver nanoparticles: green synthesis and their antimicrobial activities. Adv. Colloid Interface Sci. **145:**83–96.
11. **Zhou M, Wei Z, Qiao H, Zhu L, Yang H, Xia T.** 2009. Particle size and pore structure characterization of silver nanoparticles prepared by confined arc plasma. J. Nanomater. doi:10.1155/2009/968058.
12. **Abdel-Mohsen AM, Hrdina R, Burgert L, Abdel-Rahman RM, Hasova M, Smejkalova D, Kolar M, Pekar M, Aly AS.** 2013. Antibacterial activity and cell viability of hyaluronan fiber with silver nanoparticles. Carbohydr. Polym. **92:**1177–1187.
13. **Amato E, Diaz-Fernandez YA, Taglietti A, Pallavicini P, Pasotti L, Cucca L, Milanese C, Grisoli P, Dacarro C, Fernandez-Hechavarria JM, Necchi V.** 2011. Synthesis, characterization and antibacterial activity against Gram-positive and Gram-negative bacteria of biomimetically coated silver nanoparticles. Langmuir **27:**9165–9173.
14. **Jaiswal S, Duffy B, Jaiswal AK, Stobie N, McHale P.** 2010. Enhancement of the antibacterial properties of silver nanoparticles using beta-cyclodextrin as a capping agent. Int. J. Antimicrob. Agents **36:**280–283.
15. **Sondi I, Salopek-Sondi B.** 2004. Silver nanoparticles as antimicrobial agent: a case study on E. coli as a model for Gram-negative bacteria. J. Colloid Interface Sci. **275:**177–182.
16. **Feng QL, Wu J, Chen GQ, Cui FZ, Kim TN, Kim JO.** 2000. A mechanistic study of the antibacterial effect of silver ions on Escherichia coli and Staphylococcus aureus. J. Biomed. Mater. Res. **52:**662–668.
17. **Nover L, Scharf KD, Neumann D.** 1983. Formation of cytoplasmic heat shock granules in tomato cell cultures and leaves. Mol. Cell. Biol. **3:**1648–1655.
18. **Gupta A, Maynes M, Silver S.** 1998. Effects of halides on plasmid-mediated silver resistance in Escherichia coli. Appl. Environ. Microbiol. **64:**5042–5045.
19. **Matsumura Y, Yoshikata K, Kunisaki S-I, Tsuchido T.** 2003. Mode of bactericidal action of silver zeolite and its comparison with that of silver nitrate. Appl. Environ. Microbiol. **69:**4278–4281.
20. **Dibrov P, Dzioba J, Gosink KK, Häse CC.** 2002. Chemiosmotic mechanism of antimicrobial activity of Ag^+ in Vibrio cholerae. Antimicrob. Agents Chemother. **46:**2668–2670.
21. **Lok C-N, Ho C-M, Chen R, He Q-Y, Yu W-Y, Sun H, Tam PK-H, Chiu J-F, Che C-M.** 2006. Proteomic analysis of the mode of antibacterial action of silver nanoparticles. J. Proteome Res. **5:**916–924.
22. **Shahverdi AR, Fakhimi A, Shahverdi HR, Minaian S.** 2007. Synthesis and effect of silver nanoparticles on the antibacterial activity of different antibiotics against Staphylococcus aureus and Escherichia coli. Nanomedicine **3:**168–171.
23. **Panácek A, Kvítek L, Prucek R, Kolár M, Vecerová R, Pizúrová N, Sharma VK, Nevecná T, Zboril R.** 2006. Silver colloid nanoparticles: synthesis, characterization, and their antibacterial activity. J. Phys. Chem. B **110:**16248–16253.
24. **Pal S, Tak YK, Song JM.** 2007. Does the antibacterial activity of silver nanoparticles depend on the shape of the nanoparticle? A study of the Gram-negative bacterium Escherichia coli. Appl. Environ. Microbiol. **73:**1712–1720.
25. **Lu Z, Rong K, Li J, Yang H, Chen R.** 2013. Size-dependent antibacterial activities of silver nanoparticles against oral anaerobic pathogenic bacteria. J. Mater. Sci. Mater. Med. **24:**1465–1471.
26. **Hsin Y-H, Chen C-F, Huang S, Shih T-S, Lai P-S, Chueh PJ.** 2008. The apoptotic effect of nanosilver is mediated by a ROS- and JNK-dependent mechanism involving the mitochondrial pathway in NIH3T3 cells. Toxicol. Lett. **179:**130–139.
27. **Chopra I.** 2007. The increasing use of silver-based products as antimicrobial agents: a useful development or a cause for concern? J. Antimicrob. Chemother. **59:**587–590.
28. **Darwin KH, Miller VL.** 1999. Molecular basis of the interaction of *Salmonella* with the intestinal mucosa. Clin. Microbiol. Rev. **12:**405–428.
29. **Lahiri A, Lahiri A, Iyer N, Das P, Chakravortty D.** 2010. Visiting the cell biology of Salmonella infection. Microbes Infect. **12:**809–818.
30. **Garai P, Gnanadhas DP, Chakravortty D.** 2012. *Salmonella* enterica serovars Typhimurium and Typhi as model organisms: revealing paradigm of host-pathogen interactions. Virulence **3:**377–388.
31. **Marathe SA, Lahiri A, Negi VD, Chakravortty D.** 2012. Typhoid fever and vaccine development: a partially answered question. Indian J. Med. Res. **135:**161–169.
32. **O'Regan E, Quinn T, Pages JM, McCusker M, Piddock L, Fanning S.** 2009. Multiple regulatory pathways associated with high-level ciprofloxacin and multidrug resistance in *Salmonella* enterica serovar Enteritidis: involvement of RamA and other global regulators. Antimicrob. Agents Chemother. **53:**1080–1087.
33. **Crump JA, Barrett TJ, Nelson JT, Angulo FJ.** 2003. Reevaluating fluoroquinolone breakpoints for Salmonella enterica serotype Typhi and for non-Typhi salmonellae. Clin. Infect. Dis. **37:**75–81.

34. **Chen S, Cui S, McDermott PF, Zhao S, White DG, Paulsen I, Meng J.** 2007. Contribution of target gene mutations and efflux to decreased susceptibility of *Salmonella* enterica serovar Typhimurium to fluoroquinolones and other antimicrobials. Antimicrob. Agents Chemother. **51:**535–542.
35. **Su H-L, Lin S-H, Wei J-C, Pao IC, Chiao S-H, Huang C-C, Lin S-Z, Lin J-J.** 2011. Novel nanohybrids of silver particles on clay platelets for inhibiting silver-resistant bacteria. PLoS One **6**(6):e21125. doi:10.1371/journal.pone.0021125.
36. **Wang M-C, Lin J-J, Tseng H-J, Hsu S-H.** 2012. Characterization, antimicrobial activities, and biocompatibility of organically modified clays and their nanocomposites with polyurethane. ACS Appl. Mater. Interfaces **4:**338–350.
37. **Han D-W, Woo YI, Lee MH, Lee JH, Lee J, Park J-C.** 2012. In vivo and in vitro biocompatibility evaluations of silver nanoparticles with antimicrobial activity. J. Nanosci. Nanotechnol. **12:**5205–5209.
38. **Chiao SH, Lin SH, Shen CI, Liao JW, Bau IJ, Wei JC, Tseng LP, Hsu SH, Lai PS, Lin SZ, Lin JJ, Su HL.** 2012. Efficacy and safety of nanohybrids comprising silver nanoparticles and silicate clay for controlling *Salmonella* infection. Int. J. Nanomed. **7:**2421–2432.
39. **Huang L, Dai T, Xuan Y, Tegos GP, Hamblin MR.** 2011. Synergistic combination of chitosan acetate with nanoparticle silver as a topical antimicrobial: efficacy against bacterial burn infections. Antimicrob. Agents Chemother. **55:**3432–3438.
40. **Song K, Lee S, Park T, Lee B.** 2009. Preparation of colloidal silver nanoparticles by chemical reduction method. Korean J. Chem. Eng. **26:**153–155.
41. **Pillai ZS, Kamat PV.** 2003. What factors control the size and shape of silver nanoparticles in the citrate ion reduction method? J. Phys. Chem. B **108:**945–951.
42. **Thio BJ, Montes MO, Mahmoud MA, Lee DW, Zhou D, Keller AA.** 2012. Mobility of capped silver nanoparticles under environmentally relevant conditions. Environ. Sci. Technol. **46:**6985–6991.
43. **Rodríguez-Argüelles MC, Sieiro C, Cao R, Nasi L.** 2011. Chitosan and silver nanoparticles as pudding with raisins with antimicrobial properties. J. Colloid Interface Sci. **364:**80–84.
44. **Adler C, Corbalán NS, Seyedsayamdost MR, Pomares MF, de Cristóbal RE, Clardy J, Kolter R, Vincent PA.** 2012. Catecholate siderophores protect bacteria from pyochelin toxicity. PLoS One **7**(10):e46754. doi:10.1371/journal.pone.0046754.
45. **Wickens HJ, Pinney RJ, Mason DJ, Gant VA.** 2000. Flow cytometric investigation of filamentation, membrane patency, and membrane potential in Escherichia coli following ciprofloxacin exposure. Antimicrob. Agents Chemother. **44:**682–687.
46. **Mosmann T.** 1983. Rapid colorimetric assay for cellular growth and survival: application to proliferation and cytotoxicity assays. J. Immunol. Methods **65:**55–63.
47. **Forcet C, Ye X, Granger L, Corset V, Shin H, Bredesen DE, Mehlen P.** 2001. The dependence receptor DCC (deleted in colorectal cancer) defines an alternative mechanism for caspase activation. Proc. Natl. Acad. Sci. U. S. A. **98:**3416–3421.
48. **Eswarappa SM, Panguluri KK, Hensel M, Chakravortty D.** 2008. The yejABEF operon of *Salmonella* confers resistance to antimicrobial peptides and contributes to its virulence. Microbiology **154:**666–678.
49. **Samberg ME, Orndorff PE, Monteiro-Riviere NA.** 2011. Antibacterial efficacy of silver nanoparticles of different sizes, surface conditions and synthesis methods. Nanotoxicology **5:**244–253.
50. **Chiang CY, Schaaf HS.** 2010. Management of drug-resistant tuberculosis. Int. J. Tuberc. Lung Dis. **14:**672–682.
51. **Savard P, Gopinath R, Zhu W, Kitchel B, Rasheed JK, Tekle T, Roberts A, Ross T, Razeq J, Landrum BM, Wilson LE, Limbago B, Perl TM, Carroll KC.** 2011. First NDM-positive *Salmonella* sp. strain identified in the United States. Antimicrob. Agents Chemother. **55:**5957–5958.
52. **McAdam PR, Templeton KE, Edwards GF, Holden MT, Feil EJ, Aanensen DM, Bargawi HJ, Spratt BG, Bentley SD, Parkhill J, Enright MC, Holmes A, Girvan EK, Godfrey PA, Feldgarden M, Kearns AM, Rambaut A, Robinson DA, Fitzgerald JR.** 2012. Molecular tracing of the emergence, adaptation, and transmission of hospital-associated methicillin-resistant Staphylococcus aureus. Proc. Natl. Acad. Sci. U. S. A. **109:**9107–9112.
53. **Gnanadhas DP, Marathe SA, Chakravortty D.** 2012. Biocides: resistance, cross-resistance mechanisms and assessment. Expert Opin. Invest. Drugs **22:**191–206.
54. **Chu CY, Peng FC, Chiu YF, Lee HC, Chen CW, Wei JC, Lin JJ.** 2012. Nanohybrids of silver particles immobilized on silicate platelet for infected wound healing. PLoS One **7**(6):e38360. doi:10.1371/journal.pone.0038360.
55. **Galdiero S, Falanga A, Vitiello M, Cantisani M, Marra V, Galdiero M.** 2011. Silver nanoparticles as potential antiviral agents. Molecules **16:**8894–8918.
56. **Gupta A, Silver S.** 1998. Molecular genetics. Silver as a biocide: will resistance become a problem? Nat. Biotechnol. **16:**888.
57. **Ravindran A, Singh A, Raichur AM, Chandrasekaran N, Mukherjee A.** 2010. Studies on interaction of colloidal Ag nanoparticles with bovine serum albumin (BSA). Colloids Surf. B Biointerfaces **76:**32–37.
58. **Martinez-Gutierrez F, Olive PL, Banuelos A, Orrantia E, Nino N, Sanchez EM, Ruiz F, Bach H, Av-Gay Y.** 2010. Synthesis, characterization, and evaluation of antimicrobial and cytotoxic effect of silver and titanium nanoparticles. Nanomedicine **6:**681–688.
59. **Jones N, Ray B, Ranjit KT, Manna AC.** 2008. Antibacterial activity of ZnO nanoparticle suspensions on a broad spectrum of microorganisms. FEMS Microbiol. Lett. **279:**71–76.
60. **Tran PA, Webster TJ.** 2011. Selenium nanoparticles inhibit Staphylococcus aureus growth. Int. J. Nanomed. **6:**1553–1558.
61. **Tran N, Mir A, Mallik D, Sinha A, Nayar S, Webster TJ.** 2010. Bactericidal effect of iron oxide nanoparticles on Staphylococcus aureus. Int. J. Nanomed. **5:**277–283.
62. **Kulkarni AA, Fuller C, Korman H, Weiss AA, Iyer SS.** 2010. Glycan encapsulated gold nanoparticles selectively inhibit Shiga toxins 1 and 2. Bioconjug. Chem. **21:**1486–1493.
63. **Mariam J, Dongre P, Kothari D.** 2011. Study of interaction of silver nanoparticles with bovine serum albumin using fluorescence spectroscopy. J. Fluoresc. **21:**2193–2199.
64. **Arunachalam R, Dhanasingh S, Kalimuthu B, Uthirappan M, Rose C, Mandal AB.** 2012. Phytosynthesis of silver nanoparticles using Coccinia grandis leaf extract and its application in the photocatalytic degradation. Colloids Surf. B Biointerfaces **94:**226–230.
65. **Krasovskii V, Nagovitsyn I, Chudinova G, Savranskii V, Karavanskii V.** 2007. Interaction of gold nanoparticles with bovine serum albumin. Bull. Lebedev Phys. Inst. **34:**321–324.
66. **Yang Q, Liang J, Han H.** 2009. Probing the interaction of magnetic iron oxide nanoparticles with bovine serum albumin by spectroscopic techniques. J. Phys. Chem. B **113:**10454–10458.
67. **Lacerda SHDP, Park JJ, Meuse C, Pristinski D, Becker ML, Karim A, Douglas JF.** 2010. Interaction of gold nanoparticles with common human blood proteins. ACS Nano **4:**365–379.
68. **Yu Y, Jin G.** 2005. Influence of electrostatic interaction on fibrinogen adsorption on gold studied by imaging ellipsometry combined with electrochemical methods. J. Colloid Interface Sci. **283:**477–481.
69. **Monteiro-Riviere NA, Samberg ME, Oldenburg SJ, Riviere JE.** 2013. Protein binding modulates the cellular uptake of silver nanoparticles into human cells: implications for *in vitro* to *in vivo* extrapolations? Toxicol. Lett. **220:**286–293.
70. **Mukherjee P, Bhattacharya R, Wang P, Wang L, Basu S, Nagy JA, Atala A, Mukhopadhyay D, Soker S.** 2005. Antiangiogenic properties of gold nanoparticles. Clin. Cancer Res. **11:**3530–3534.
71. **Hindi KM, Ditto AJ, Panzner MJ, Medvetz DA, Han DS, Hovis CE, Hilliard JK, Taylor JB, Yun YH, Cannon CL, Youngs WJ.** 2009. The antimicrobial efficacy of sustained release silver-carbene complex-loaded l-tyrosine polyphosphate nanoparticles: characterization, *in vitro* and *in vivo* studies. Biomaterials **30:**3771–3779.
72. **Zolghadri S, Saboury AA, Golestani A, Divsalar A, Rezaei-Zarchi S, Moosavi-Movahedi AA.** 2009. Interaction between silver nanoparticle and bovine hemoglobin at different temperatures. J. Nanopart. Res. **11:**1751–1758.